공학석사학위논문

미세 유체 소자를 이용한 체외 림프 전이 모델

Microfluidic *In Vitro* Model of Lymphatic Metastasis

2018년 2월

서울대학교 대학원

기계항공공학부

손 경 민

Abstract

Microfluidic *In Vitro* Model of Lymphatic Metastasis

Kyungmin Son

School of Mechanical and Aerospace Engineering

The Graduate School

Seoul National University

Lymphatic vessels are closely involved in various diseases including inflammation and metastasis. However, elucidating the mechanisms of lymphatic function in physiological and pathological condition has been hampered by lack of reliable *in vitro* model recapitulating the complex in vivo environment of lymphatic vessels. In this study, a microfluidic platform that reconstitutes the three-dimensional lymphatic vascular network with luminal accessibility is presented. Fibroblasts together with pro-lymphangiogenic factors successfully supported the development of vascular network from primary human lymphatic endothelial cells. The

vascular formation was further promoted by the appropriate speed of flow induced by hydrostatic pressure difference. The vascular network was perfused only when LECs were patterned separately with fibroblasts and flow was applied. The perfused network exhibited basic characteristics of in vivo lymphatic vessels, and it was maintained intact at least for 5 days only with basal medium. After vessel perfusion, cancer cells introduced into the device moved into the vascular network and stably adhered to the inside of vessels. This study provides a biomimetic 3D in vitro model that allows for studying the function of lymphatic endothelium in cancer metastasis and immune response.

Keywords: Lymphatic vessel, Perfused vessel, Metastasis, Microfluidics

Student Number: 2016-20656

Contents

List of figures

Mixture of LECs and fibroblasts are introduced into central channel. (B) LECs are introduced into central channels, and fibroblasts are injected into side channels.

Figure 3.2 Vascular formation under different types and concentrations of fibroblasts. (A) LECs were cultured 48 hours with pLFs only (i), fibroblasts only (ii). With pLFs cocktail, LECs were mixed with dermal fibroblasts (iii), or lung fibroblasts (iv). LECs were separately cultured with dermal fibroblasts (v), or lung fibroblasts (vi). Scale bars, 200 μm. (B) Vessel area in the central channel when fibroblasts were mixed with LECs. (C) Vessel area when fibroblasts were patterned in side channels. Error bars represent SEM from at least 5 devices, $*p<0.05$ and $**p<0.01$ in unpaired two-tailed Student's T-tests.

Figure 3.3 Vascular formation under different speed of interstitial flow. (A) LECs were cultured 48 hours under static condition or flow condition of 20 μL, 40 μL, 80 μL media volume difference. Scale bars, 200 μm. (B) Vessel area in the central channel when fibroblasts were mixed with LECs. (C) Vessel area when fibroblasts were patterned in side channels. Error bars represent SEM calculated from 6 devices, $*p<0.05$, $**p<0.01$, and $****p<0.0001$.

Figure 3.4 Day-by-day vascular formation in optimized condition. (A) LECs were cultured in mixed condition. (B) LECs were cultured in separated condition. Scale bars, 200 μm.

Figure 3.5 Verifying vessel perfusion by introducing microbeads. (A) LECs were mixed with fibroblasts, and cultured under static (i) and flow (ii) condition. LECs were separated with fibroblasts under static (iii) and flow (iv) condition. On day 5, microbeads (7 μm, green) were introduced into the microfluidic device having 20 μL volume difference across the central channel. Scale bars, 200 μm. (B) The

number of perfused positions which allow the microbeads to flow into the vascular network at the interposts under four conditions. Error bars represent SEM from at least 8 devices, $^{**}p<0.01$, $^{***}p<0.001$, and $^{****}p<0.0001$.

Figure 3.6 Characterization of engineered 3D lymphatic vascular network. (A, B) Confocal images of major components of basement membrane of lymphatic vessels, laminin (red) or collagen IV (purple). (C) Master regulator of lymphatic morphogenesis, prox1 (red), was expressed in the nuclei of most LECs in lymphatic vessels. Scale bars, 100 μm.

Figure 3.7 Cancer cells inside perfused lymphatic vessels. After 5 days culture, melanoma cells introduced into the microfluidic device moved into the perfused lymphatic vessels and adhered to the apical side of the vessels. (A) Single cells in the vessels. Scale bars, 200 μm. (B) Aggregated cells in the vessels. Scale bars, 100 μm.

Chapter 1. Introduction

Lymphatic vessels, together with blood vessels, constitute the circulatory system which transport fluids, nutrients, molecules and cells within the body to maintain homeostasis in the living organisms. Since lymphatic system makes a significant contribution to fluid drainage from the tissue and the migration of immune cells, lymphatic abnormalities give rise to various diseases such as lymphedema and inflammation [1]. Lymphatic metastasis, characterized by the spread of cancer cells through a lymphatic vessel to a second site, have been seriously implicated in the presence of diverse negative factors in cancer patients [2, 3]. The development of metastasis caused by the entrapment of cancer cells within lymphatic often heralds progression to regional and systemic disease [4], which emphasizes the understanding of the characteristics of lymphatic metastasis for cancer treatment and drug discovery. Lymphatic vessels also play critical roles in regulating immune reactions [5]. They influence the immune cell trafficking and migration through the close and reciprocal interaction with immune cells both in physiological and pathological conditions. These phenomena are related to the cellular interaction between the lymphatic vessel and the cells inside the vessel, however, the mechanisms by which lymphatic endothelial cells (LECs) modulate the transport, proliferation, and function of cells are poorly understood [6, 7]. The complexity of observing in vivo cellular dynamics inside the lymphatic vessel advocates the necessity of in vitro modeling of the corresponding process. Therefore, engineering biologically relevant lymphatic system consisting of LECs

is first to be realized to further investigate the regulatory mechanisms in the native lymphatic network.

A lot of research on the function of endothelium depends on simplified models to reduce the complexity of the experiment. Coverslip or membrane with endothelial cells provides 2D monolayer model [8–10]. A few hours or days after dropping cancer cells or immune cells on the monolayer, cells on the layer or at the opposite side of the chamber is imaged to quantify the number of attached cells or extravasated cells. Although 2D monolayer model is a powerful tool to elucidate specific aspects of the interaction, this model lacks the extracellular matrix and 3D vessel structure seen in native tissues, having weak relevance to the in vivo vessel. Employing cylindrical template [11, 12], soft lithography [13, 14], 3D printing technique [15], or other techniques [16, 17] allowed to generate channel network embedded in PDMS or hydrogel, which is followed by introducing ECs into the channel to form an artificial vascular network. This model provides perfusable vascular network with inlets and outlets, capable of introducing other cells to interact with 3D vessel structure. Recently developed microfluidic devices enable to induce self-assembly of ECs into the vascular network by providing in vivo-like microenvironment including hydrogel, stromal cells, chemical gradient and interstitial flow. In addition, patterning cells and media generated self-assembled perfusable network in microchannels [18–23]. This network facilitates the observation of physiologically relevant events in real time, and several researchers have reported the permeability test and cancer extravasation using the models. Different from blood vessel network using blood endothelial cells (BECs), however, there has been almost no research constructing perfusable lymphatic

vascular network [24] since microenvironmental factors for the growth of lymphatic endothelium have not yet been firmly established. Without adopting proper platform, only 2D monolayer models [25–27], pre-defined vessel model [28] or 3D constructs model with non-perfused vasculature [29–33] have been often reported. In the absence of a 3D perfusable lymphatic model, the processes of extravasation and cancer growth in the native vessel cannot be live-imaged and analyzed.

The present study aims to engineer lymphatic vascular network which is both perfused and physiologically relevant with in vivo lymphatic system. Optimization process of cell culture conditions including biochemical, biophysical factors and cell seeding configuration is described for making well-developed and open luminal structure capable of access to the inside of the vascular network. The stability and the characteristics of the perfused lymphatic vasculature are verified by immunostaining in diverse conditions. A preliminary experiment with cancer cells is performed to show the potential of the model to investigate the cell-lymphatics interaction inside the lymphatic vessel.

Chapter 2. Materials and Methods

2.1 Microfluidic device fabrication

Master mold of microfluidic device was fabricated by photolithography for 200 μm height of positive relief structure on the silicon wafer using negative photoresist SU-8. The 2D design of the device was established by AutoCAD to have 1000 μm width of the central channel, which is same with previously designed one by our group [19] (Figure 2.1). The microfluidic platform was made by soft lithography using Polydimethylsiloxane (PDMS, Sylgard 184, Dow Corning). A prepolymer mixture of PDMS and curing agent mixed in the ratio of 10:1 (w/w) was poured onto the master mold and degassed in a vacuum under 0.2 bar absolute pressure. After 30 min on 85 ℃ hot plates for curing, the PDMS having negative replica structure was peeled off from the master mold. Four media reservoirs and six small holes for hydrogel injection were punched using 6mm biopsy punch and 1mm syringe needle, respectively. The device was bonded with glass coverslip by treating oxygen plasma for 1 min and incubated in a 75 ℃ dry oven for at least 48 hours to restore PDMS to be hydrophobic.

2.2 Cell culture

Human Umbilical Vein Endothelial Cells (HUVECs, Lonza) and Human dermal lymphatic microvascular endothelial cells (HMVECs-dLyAd, Lonza) were cultured in endothelial basal medium (EBM-2, Lonza) supplemented with EGM-2 and EGM-2 MV Bulletkit respectively, and used at passage 6. Normal human lung fibroblasts (NHLFs, Lonza) and Dermal fibroblasts (DFs, CEFO) were cultured in fibroblast growth medium (FGM-2, Lonza) and used at passages 6. A375SM melanoma cells were grown in Dulbecco's modified Eagle medium (DMEM, Hyclone) supplemented with 10% fetal bovine serum and 1% Penicillin/Streptomycin. All cells were maintained at 37 ℃ and 5% CO2 atmosphere in a humidified incubator. HUVECs and HMVECs were harvested for experiments before reaching confluent.

2.3 Vasculogenesis cell seeding

10 mg/mL fibrinogen (F8630, 2.5 mg/mL final concentration, Sigma-Aldrich) with aprotinin (A1153, 0.15 U/ml final concentration, Sigma-Aldrich) was prepared in phosphate buffered saline (Hyclone). After detached from the cell culture dish, fibroblasts and endothelial cells were resuspended in new medium. In mix culture condition, the two side channels were filled with 2.5 mg/mL acellular fibrinogen mixed with thrombin (T4648, 1 U/mL final concentration). Then fibroblasts and LECs are mixed at a ratio of 0:1, 0.5:1 and 1:1, suspended in fibrinogen to have a LECs' concentration of 4×10^6 cells/mL, and then injected

into the central channel. In separate culture condition, the side channels and the central channels were filled with fibroblasts ($2{,}4{,}8 \times 10^6$ cells/mL) and LECs (4×10^6 cells/mL), respectively. The device was left 3 min at room temperature for fibrin polymerization after the gel injection, and either EGM-2 MV or EGM-2 MV supplemented with pro-lymphangiogenic factors (pLFs) was loaded to fill the medium channels and the reservoirs. The pLFs cocktail was previously reported by our group [34], which includes 25 ng/mL for vascular endothelial growth factor-A (VEGF-A, R&D Systems), VEGF-C (R&D Systems), basic fibroblast growth factor (bFGF, Invitrogen), 50 ng/mL for Endocan (R&D Systems) and 500 μM for sphingosine-1-phosphate (S1P, Sigma-Aldrich) to promote the growth of LECs. For experiments in flow condition, the hydrostatic pressure difference between two medium channels is applied every 12h to induce interstitial flow across the central channel. The region of applied flow speed corresponds to the speed of interstitial flow measured in vivo [35].

2.4 Vessel perfusion verification

Fluorescent polystyrene beads with a diameter of 7 μm were suspended in PBS to confirm that the lymphatic vascular networks formed in the microfluidic device were perfusable. At 5 days of vessel formation, all reservoirs were aspirated and 20 μl of bead solution was loaded on one side of the reservoir, inducing pressure driven bead flow through perfused vessels. The vessels at the interposts were counted as open when the vessels allowed the beads to flow into the network. The network

was considered perfused when beads introduced in one media channel were transported across the central channel.

2.5 Cancer cell introduction

After 5 days of LECs injection, A375SM melanoma cells were fluorescently labeled with CellTracker Red (2 μM, Molecular Probes) and harvested to be resuspended in EBM-2 at the concentration of 1.5×10^6 cells/mL. All four reservoirs of the microfluidic devices were aspirated, and 5 μL of the cell suspension was added to one reservoir to make cells flow into the network. Cancer cells then adhere onto the apical side of lymphatic endothelium, followed by filling the reservoirs with fresh EBM-2 medium and keeping the device in an incubator for 5 days.

2.6 Immunostaining and Imaging

Samples were fixed by replacing culture medium with 4% paraformaldehyde (Biosesang) for 15 min, permeabilized with 0.15% Triton X-100 (Sigma-Aldrich) for 20 min, and blocked by 3% bovine serum albumin (Santa Cruz Biotechnology) for 1 h at room temperature. Mouse monoclonal antibody specific for human CD31 (clone WM59, BioLegend) marks the blood vessel, and rat monoclonal antibody for human podoplanin (clone NC-08, BioLegend) is used for lymphatic vessel marker. Rabbit polyclonal antibodies against human laminin (Abcam) and human collagen IV (Abcam) is added to visualize basement membrane. Samples were

incubated with fluorescence-conjugated primary antibodies (CD31; 1:200, podoplanin; 1:200) or non-conjugated primary antibodies (laminin; 1:100, collagen IV; 1:100) overnight at 4 ℃, subsequently treated with appropriate secondary antibodies with a fluorescent dye. For staining of F-actin and nucleus, samples were incubated for 2 h with Alexa Fluor-conjugated phalloidin and Hoechst 33342 (Molecular Probes) at 1:200 and 1:1000 dilution, respectively. After the incubation, the samples were washed three times with PBS and stored at a 4 ℃ refrigerator until imaging. For acquiring z stack images of 3D structures, stained samples were imaged by Olympus FV1000 confocal microscope with x10, x20 and x40 lenses. Images were taken in the identical settings when the fluorescence intensity values under different conditions need to be quantitatively measured.

2.7 Quantification and statistical analysis

To quantify the area of the lymphatic vascular network, podoplanin in lymphatic endothelium was stained and imaged by confocal microscopy. The images were analyzed by Fiji (http://fiji.sc/Fiji). 3D stacks of vascular networks images were z-projected and converted to binary images. After reducing background noise, the appropriate threshold was applied to the images to measure the fluorescent area within the region of interest. Statistical significance was evaluated by unpaired two-tailed Student's T-tests, with the threshold defined as *$p < 0.05$; **$p < 0.01$; ***$p < 0.001$; ****$p < 0.0001$; ns (not significant) $p > 0.05$. Error bars mean standard error of the mean (SEM).

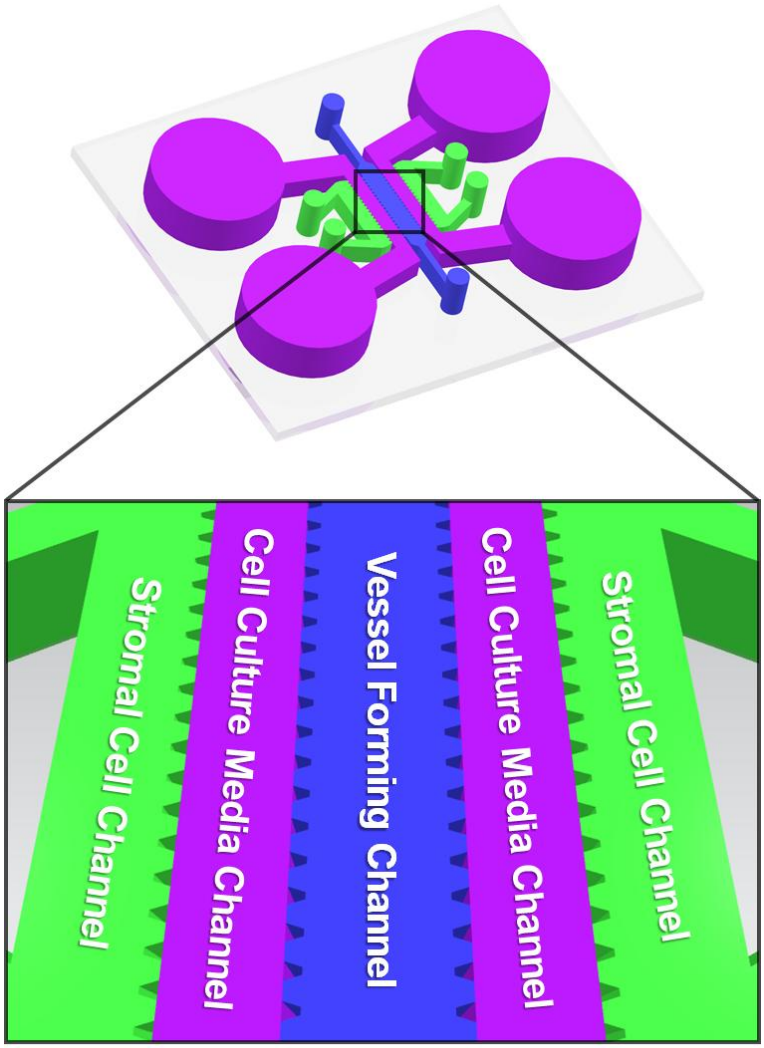

Figure 2.1 Schematic of the microfluidic device. The device consists of five channels which are separated by arrays of microposts.

Chapter 3. Results

3.1 Cultural condition optimization

HDLECs were used as LECs, and fibroblasts were adopted as stromal cells to induce the growth of LECs. A mixture of fibroblasts and LECs were injected into central channels, or fibroblasts were injected into side channels and LECs were introduced into central channels for vascular network development (Figure 3.1). To promote the formation of lymphatic vessels, optimal cell types, the density of fibroblasts, and flow speed were tested.

3.1.1 Fibroblasts type and density optimization

LECs were cultured with or without previously tested pro-lymphangiogenic factors including VEGF-A, VEGF-C, bFGF, endocan, and S1P, and two kinds of fibroblasts, NHLFs and DFs, for 4 days. Figure 3.2 shows that pLFs cocktail alone and fibroblasts alone are not enough to induce vessel formation. When combined with pLFs, both fibroblast types could develop lymphatic vessels. To reduce the number of experimental conditions, the concentration of LECs was fixed at 4

mil/ml and the maximum concentration inside the microchannel was set at 8 mil/ml. Therefore 2 and 4 mil/ml of fibroblasts were used in the mix condition and 2, 4, and 8 mil/ml of fibroblasts were used in the separate condition. Unlike separate culture conditions where no significant difference of vessel area was found between two cells, the formation of the lymphatic vessel was more promoted by LFs than DFs in every concentration. In case of concentration, the higher number of fibroblasts induces the larger area of the lymphatic vessel. As a result, LFs of 4 mil/ml in mixed condition and 8 mil/ml of separate condition were adopted in later experiments.

3.1.2 Flow speed optimization

The previous study showed that lymphatic sprouting is promoted by interstitial flow which provides mechanical stimulus to LECs. To confirm that lymphatic network development is also enhanced by interstitial flow, flow conditions were compared with the static condition. In a microfluidic device, flow across the central channel is generated by making media volume difference between left and right reservoirs. Three kinds of volume difference (Δ20 μL, Δ40 μL, Δ80 μL) were tested for the experiment (Figure 3.3). Lymphatic vessels in mix culture showed no significant difference in growth below Δ40 μL, but vessels in separate culture showed enhanced growth by the increase of volume difference below Δ40 μL. On the contrary, the area of vessels in both conditions was minimized under Δ80 μL, indicating that too much mechanical stimulus hampers

lymphatic growth. According to the data, volume differences of Δ20 μL in mix culture and Δ40 μL in separate culture were decided to be applied in later experiments.

3.2 Perfusable network formation

In optimally adjusted condition, LECs were cultured in the mix or separate configuration to form perfusable vascular network. Two configurations yielded different shapes of the vascular network in 4 days development (Figure 3.4). Vessels in separate condition are thicker and more connected each other, and the networks were more stretched to the outside, occupying the interposts area. To verify that the networks are perfused, 7 μm microbeads were introduced into the media channel on day 5. Figure 3.5 shows that the beads flew into the network and moved across the central channel only in separate condition with the flow. Actually, in about 9 experiments, no vessels in mix condition were perfused regardless of flow, and only one of eight networks in separate, static condition was perfused. On the contrary, eight of nine networks were perfused in separate, flow condition, indicating that cell seeding configuration and presence of interstitial flow play a critical role in making vessels perfusable.

3.3 Characteristics of lymphatic vascular network

To confirm that lymphatic vessels formed by HDLECs and LFs in the microfluidic device have similar characteristics of in vivo vessels, prox1, laminin, and collagen IV were stained and observed. As seen in Figure 3.6, prox1, a regulator of lymphatic morphogenesis, was expressed in most of LECs comprising the vascular network. In addition, images of laminin and collagen IV show perforated vessels, which reflects in vivo lymphatic vessels having a discontinuous basement membrane.

3.4 Cancer cells introduction and attachment

It takes time to see the interaction between cancer cells and lymphatic vessels, and the growth factors and serum proteins contained in the medium could interfere the analysis of pure interaction between two. Therefore, the perfused vascular network should be maintained intact within a period with basal medium for the experiment introducing cancer cells. To confirm this, LECs were cultured 5 days with complete medium containing serum and pLFs to form perfusable network, and cultured with basal medium without any additional factors for next 5 days. On day 5, melanoma cells (A375SM) which metastasize through lymphatic vessels were introduced into the network and incubated with basal medium for 5 days. Figure 3.7 shows that perfused vascular networks in basal medium did not regress. In addition, single or aggregated cancer cells were firmly adhered to the lymphatic vessels, indicating that the lymphatic vascular network provides a reliable model for lymphatic metastasis.

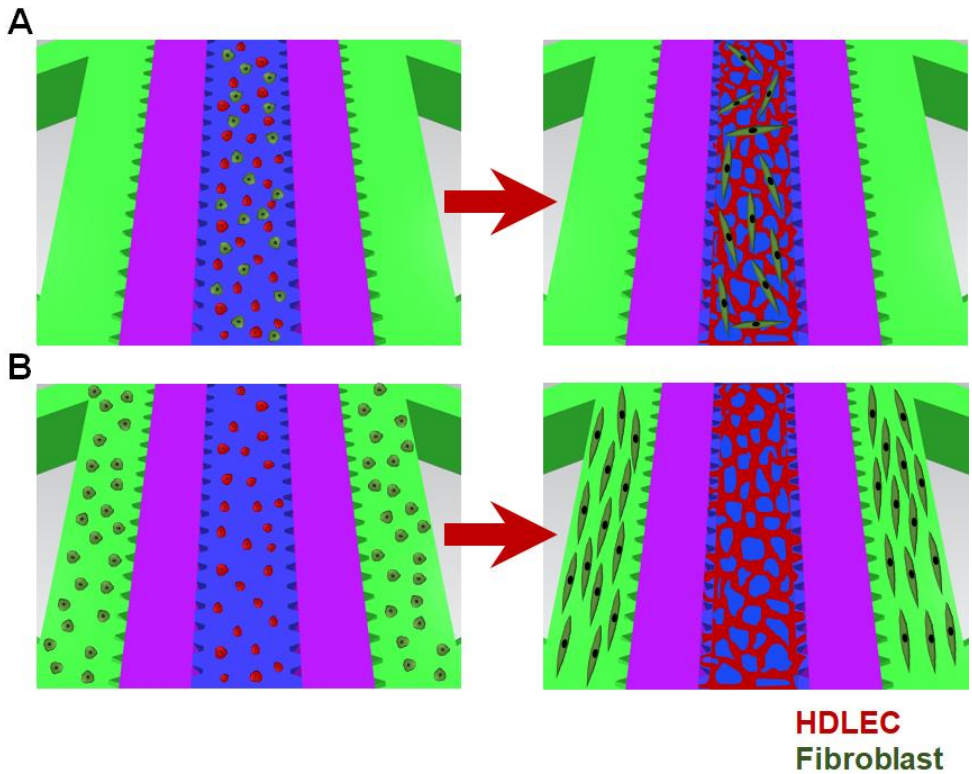

Figure 3.1 Schematic diagram of lymphatic vascular network formation. (A) Mixture of LECs and fibroblasts are introduced into central channel. (B) LECs are introduced into central channels, and fibroblasts are injected into side channels.

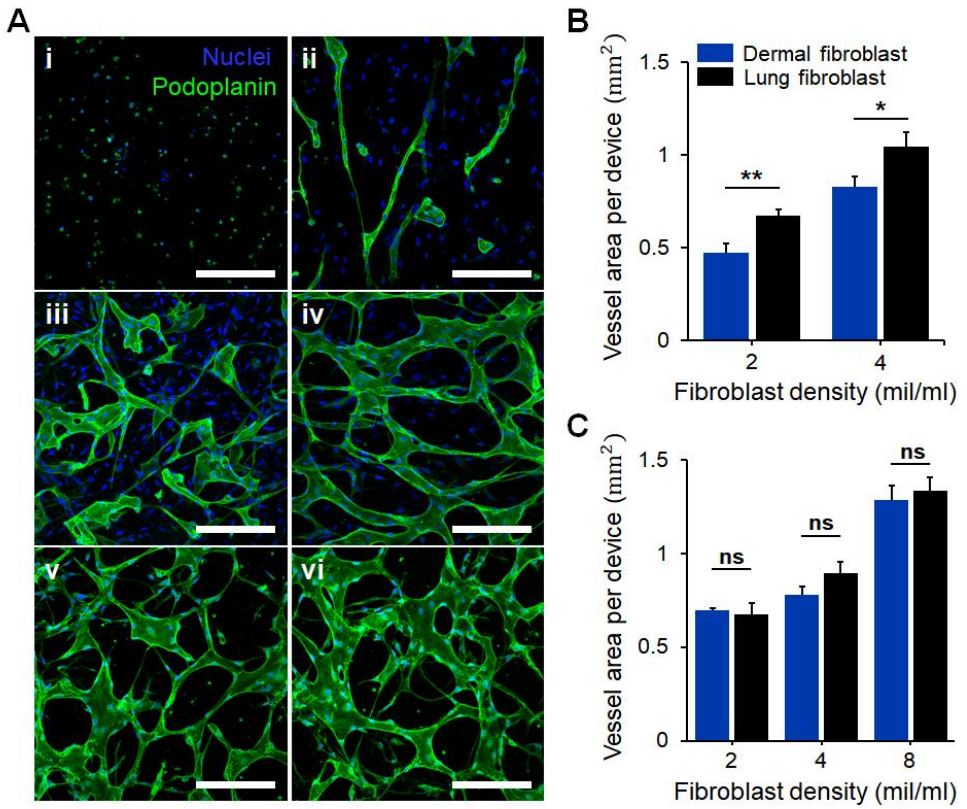

Figure 3.2 Vascular formation under different types and concentrations of fibroblasts. (A) LECs were cultured 48 hours with pLFs only (i), fibroblasts only (ii). With pLFs cocktail, LECs were mixed with dermal fibroblasts (iii), or lung fibroblasts (iv). LECs were separately cultured with dermal fibroblasts (v), or lung fibroblasts (vi). Scale bars, 200 μm. (B) Vessel area in the central channel when fibroblasts were mixed with LECs. (C) Vessel area when fibroblasts were patterned in side channels. Error bars

represent SEM from at least 5 devices, *p<0.05 and **p<0.01 in unpaired two-tailed Student's T-tests.

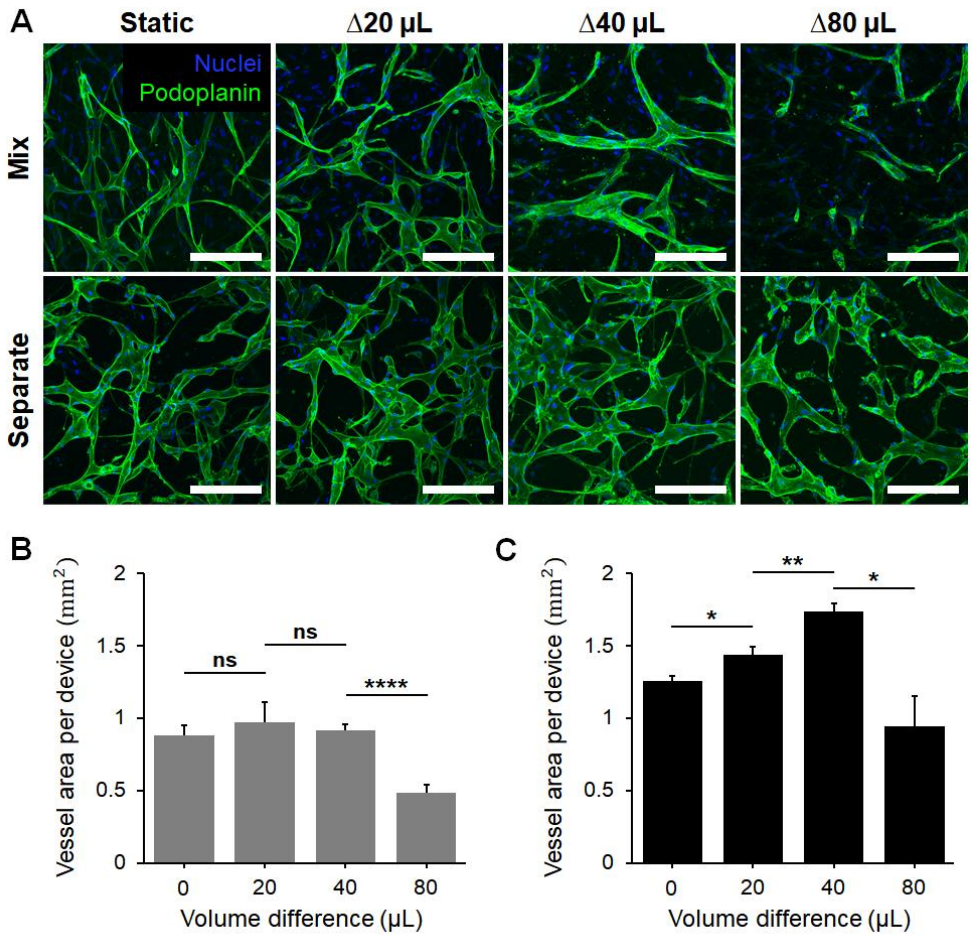

Figure 3.3 Vascular formation under different speed of interstitial flow. (A) LECs were cultured 48 hours under static condition or flow condition of 20 μL, 40 μL, 80 μL media volume difference. Scale bars, 200 μm. (B) Vessel area in the central channel when fibroblasts were mixed with LECs. (C) Vessel area when fibroblasts were patterned in side channels. Error bars represent SEM calculated from 6 devices, *p<0.05,

**p<0.01, and ****p<0.0001.

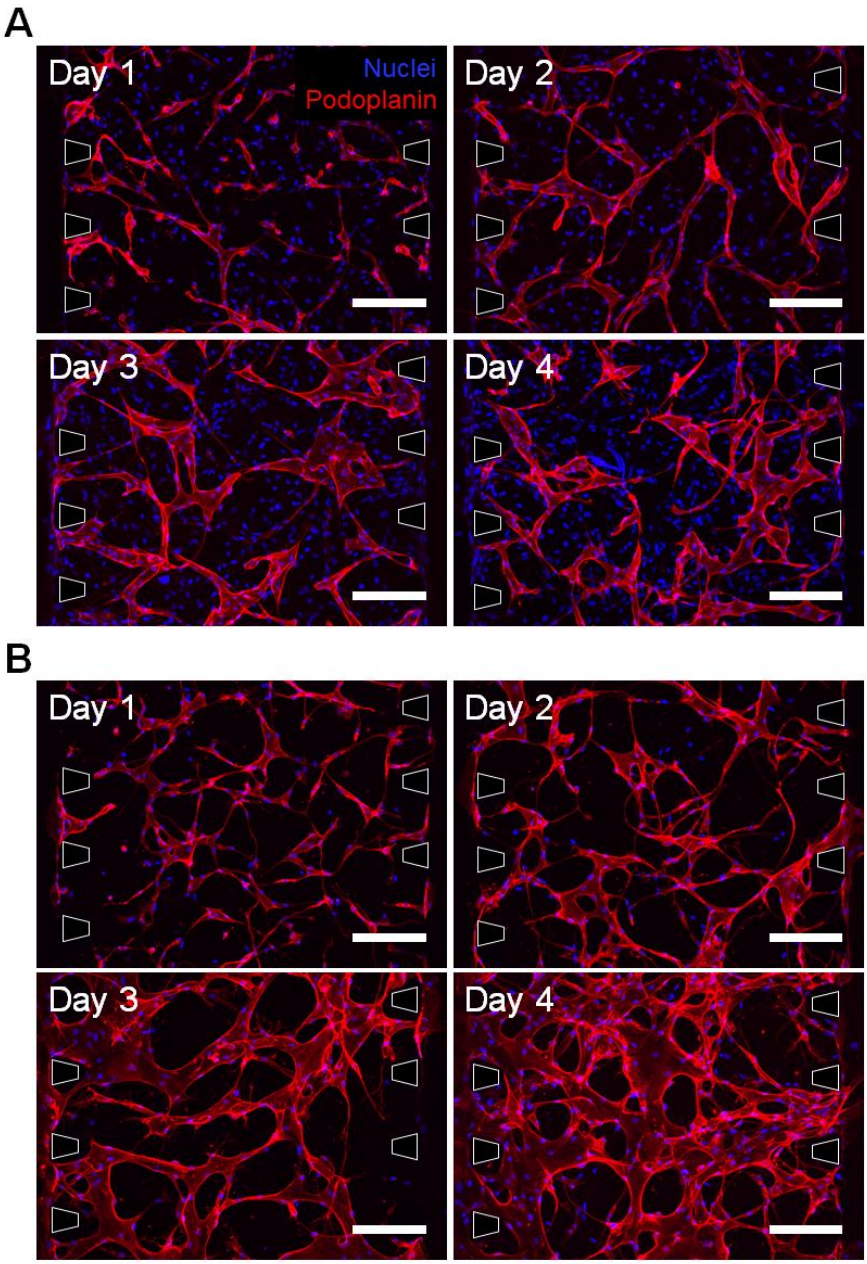

Figure 3.4 Day-by-day vascular formation in optimized condition. (A) LECs were

cultured in mixed condition. (B) LECs were cultured in separated condition. Scale bars, 200 μm.

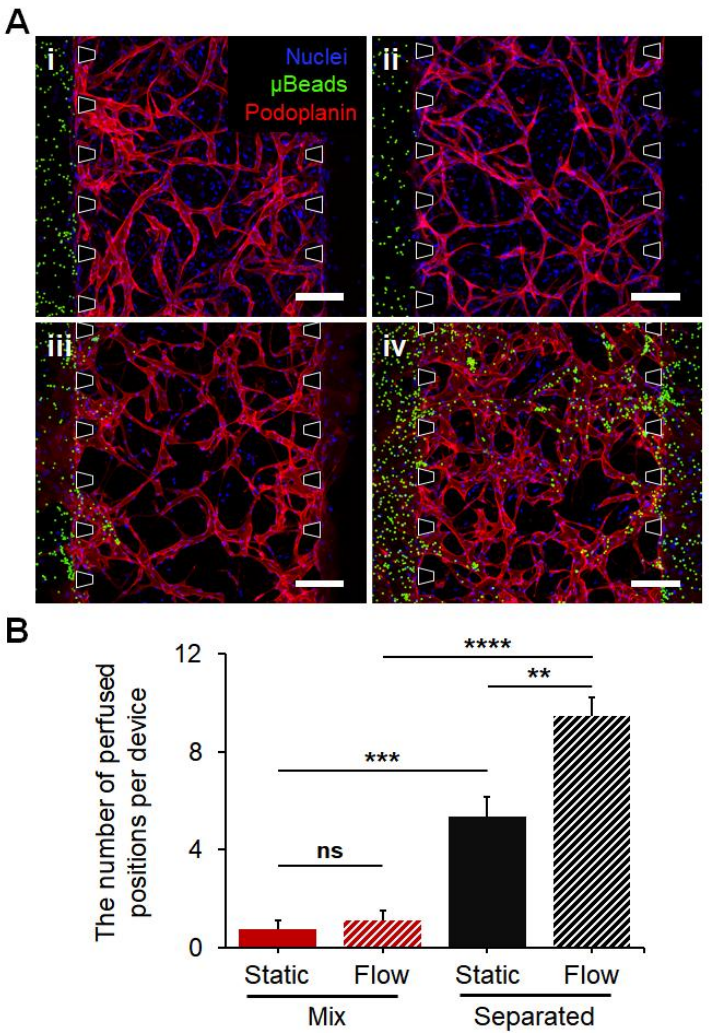

Figure 3.5 Verifying vessel perfusion by introducing microbeads. (A) LECs were mixed with fibroblasts, and cultured under static (i) and flow (ii) condition. LECs were separated with fibroblasts under static (iii) and flow (iv) condition. On day 5, microbeads (7 μm, green) were introduced into the microfluidic device having 20 μL volume difference across the central channel. Scale bars, 200 μm. (B) The number of

perfused positions which allow the microbeads to flow into the vascular network at the interposts under four conditions. Error bars represent SEM from at least 8 devices, $^{**}p<0.01$, $^{***}p<0.001$, and $^{****}p<0.0001$.

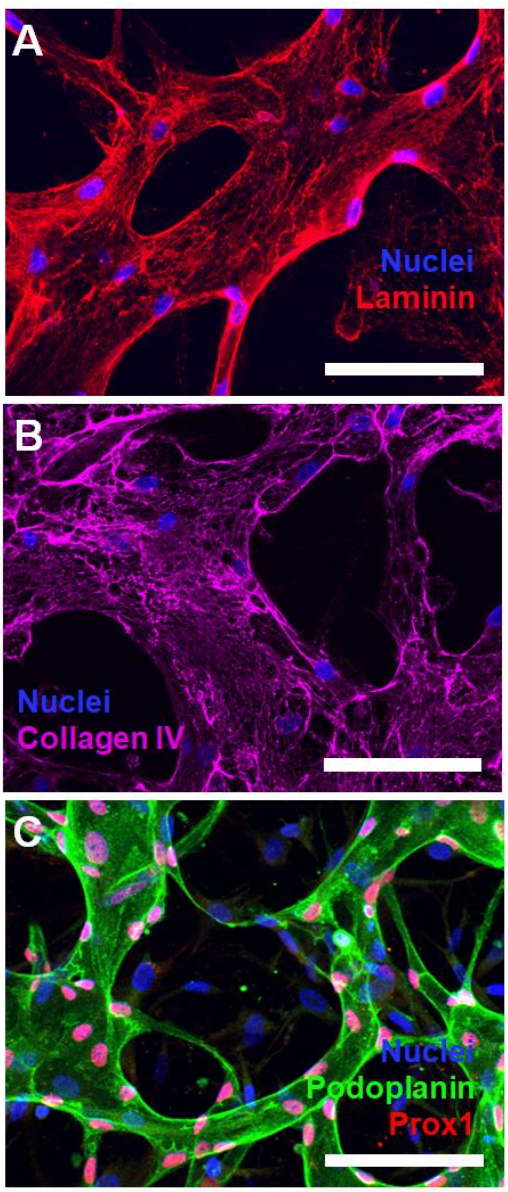

Figure 3.6 Characterization of engineered 3D lymphatic vascular network. (A, B) Confocal images of major components of basement membrane of lymphatic vessels,

laminin (red) or collagen IV (purple). (C) Master regulator of lymphatic morphogenesis, prox1 (red), was expressed in the nuclei of most LECs in lymphatic vessels. Scale bars, 100 μm.

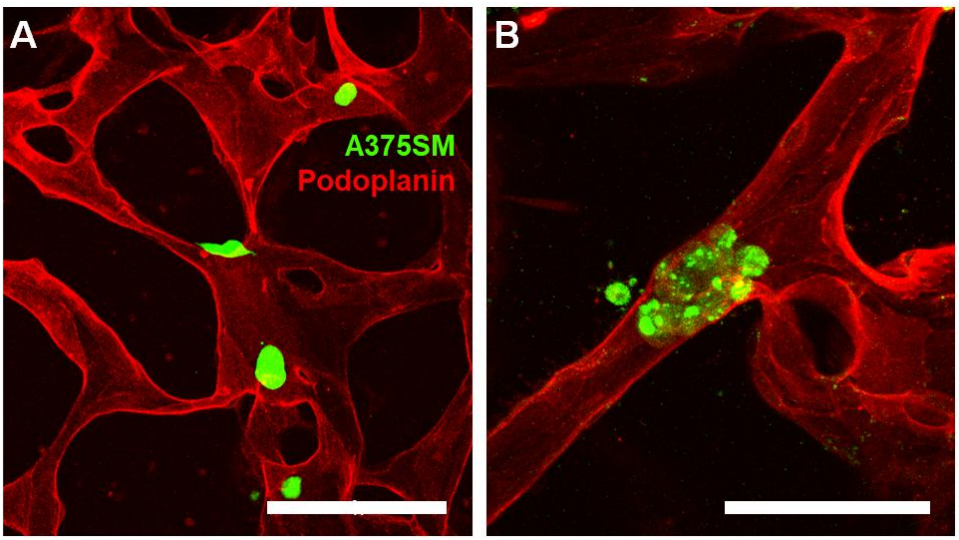

Figure 3.7 Cancer cells inside perfused lymphatic vessels.. After 5 days culture, melanoma cells introduced into the microfluidic device moved into the perfused lymphatic vessels and adhered to the apical side of the vessels. (A) Single cells in the vessels. Scale bars, 200 μm. (B) Aggregated cells in the vessels. Scale bars, 100 μm.

Chapter 4. Discussion

This study presents the process of engineering 3D perfusable lymphatic vascular network using human cells in the microfluidic device. To make the LECs grow into the vascular network well, both fibroblasts and pro-lymphangiogenic factors are required. This is different from blood vessel where fibroblasts are enough for the vascular development. In flow condition, appropriate mechanical stress induced by interstitial flow is also necessary to promote the lymphatic vessel formation, which agrees with the increase of prox1 and Ki-67 in flow condition previously reported by our group [34]. Although the formation of the lymphatic vascular network was impeded under the volume difference of Δ80 μL, that of blood vascular network was further promoted under the same condition, indicating that two endothelial cells have different sensitivity to the flow.

In two configurations, perfusable vascular networks were made only in separate culture condition. Two conditions showed different responses to the flow, meaning that vascular development in mix condition was not significantly promoted by the flow. Unlike separate condition, fibroblasts are positioned in the central channel where the interstitial flow is applied. Therefore, it is expected that fibroblasts stimulated by flow had a negative influence on the growth of LECs. This expectation can be related to the fibroblast differentiation [36], which might

secrete negative regulator of lymphatic growth such as transforming growth factor-β1 [37–40]. The exact mechanism of the phenomenon needs to be further investigated. Aside from the disruption of lymphatic growth, LECs mixed with fibroblasts are not induced to grow to the interposts of the central channel since the concentration of growth factors and proteins made by fibroblasts are decreasing along the direction outward from the channel. This shows that culturing cells only with hydrogel scaffold which many researchers have used is not effective to make perfusable vessels. Although adopting cell sheets with an endothelial layer on top and bottom layer also makes perfusable vessel, it has a limitation on tissue thickness. The disadvantages of established methods demonstrate the necessity of cell patterning using microfluidics.

Unlike monolayer model, lymphatic vessels formed in the microfluidic device have perforated basement membrane which is similar to the native vessels, and they were stably maintained with basal medium at least 5 days. These features allow this model to study in vivo-like response to external factors such as cancer cells or immune cells. The experiment introducing cancer cells into the vascular networks showed that cells were firmly attached to the vessel, making it possible to see the interaction between two. Using this model, next step will be the analysis of the difference in responses of cancer or immune cells to the blood vessels and lymphatic vessels. Also, based on the culture condition making a lymphatic vascular network, BECs and LECs will be co-cultured in one channel to engineer separate network. Since the culture method does not require stromal cell-endothelial cell contact for the vascular network formation, this model will be distinguished from previous research.

Chapter 5. Conclusion

By optimizing culture condition, 3D lymphatic vascular network originating from human cells was made on the multichannel microfluidic device. Introducing microbeads in the microfluidic device showed that the network becomes perfused when LECs and fibroblasts are separately patterned and moderate interstitial flow is applied. Expression of prox1 and discontinuous basement membrane proteins certified that the vessels closely mimic in vivo lymphatic vessel. The perfused vessels remain intact for 5 days with basal medium, and cancer cells introduced to the device stably adhered to the apical side of the vessels. This study demonstrates the potential of the model for use in investigating the function of lymphatic endothelium in cancer development, studying the mechanism of lymphatic metastasis, and developing drug for cancer treatment.

Bibliography

[1] Alitalo, K., T. Tammela, and T. V Petrova, *Lymphangiogenesis in development and human disease.* Nature, 2005. **438**(7070):p. 946–953.

[2] Stacker, S. A., et al., *Lymphangiogenesis and lymphatic vessel remodelling in cancer*. Nature Reviews Cancer, 2014. **14**(3):p. 159–172.

[3] Karaman, S. and M. Detmar, *Mechanisms of lymphatic metastasis*. Journal of Clinical Investigation, 2014. **124**(3):p. 922.

[4] Beasley, G. and D. Tyler, *In-transit Melanoma Metastases: Incidence, Prognosis, and the Role of Lymphadenectomy.* Annals of Surgical Oncology, 2015. **22**(2):p. 358–360.

[5] Kataru, R. P., Y. G. Lee, and G. Y. Koh, *Interactions of immune cells and lymphatic vessels*. Developmental Aspects of the Lymphatic Vascular System, 2014:p. 107–118.

[6] Lee, E., N. B. Pandey, and A. S. Popel, *Lymphatic endothelial cells support tumor growth in breast cancer*. Scientific Reports, 2014. **4**:p. 5853

[7] Shah, T., et al., *Lymphatic endothelial cells actively regulate prostate cancer cell invasion*. NMR in Biomedicine, 2016. **29**(7):p. 904–911.

[8] Li, Y. H. and C. Zhu, *A modified Boyden chamber assay for tumor cell transendothelial migration in vitro*. Clinical and Experimental Metastasis,

1999. **17**(5):p. 423–429.

[9] Dong, C., et al., *In vitro characterization and micromechanics of tumor cell chemotactic protrusion, locomotion, and extravasation*. Annuals of Biomedical Engineering, 2002. **30**(3):p. 344–355.

[10] Chotard-Ghodsnia, R., et al., *Morphological analysis of tumor cell/ endothelial cell interactions under shear flow*. Journal of Biomechanics, 2007. **40**(2):p. 335–344.

[11] Chrobak, K. M., D. R. Potter, and J. Tien, *Formation of perfused, functional microvascular tubes in vitro*. Microvascular Research, 2006. **71**(3):p. 185–196.

[12] Bogorad, M. I., et al., *in vitro microvessel models*. Lab on a Chip, 2015. **15**(22):p. 4242–4255.

[13] Zheng, Y., et al., *In vitro microvessels for the study of angiogenesis and thrombosis*. Proceedings of the National Academy of Sciences, 2012. **109**(24):p. 9342–9347.

[14] Li, X., et al., *In vitro recapitulation of functional microvessels for the study of endothelial shear response, nitric oxide and [Ca2+] I*. PLoS One, 2015. **10**(5):p. e0126797.

[15] Miller, J. S., et al., *Rapid casting of patterned vascular networks for perfusable engineered three-dimensional tissues*. Nature Materials, 2012. **11**(9):p. 768–774.

[16] Heintz, K. A., et al., *Fabrication of 3D biomimetic microfluidic networks in hydrogels*. Advanced Healthcare Materials, 2016. **5**(17):p. 2153–2160.

[17] Zhang, B., et al., *Biodegradable scaffold with built-in vasculature for*

organ-on-a-chip engineering and direct surgical anastomosis. Nature Materials, 2016. **15**(6):p. 669–678.

[18] Whisler, J. A., M. B. Chen, and R. D. Kamm, *Control of perfusable microvascular network morphology using a multiculture microfluidic system*. Tissue Enineering Part C: Methods, 2012. **20**(7):p. 543–552.

[19] Kim, S., et al., *Engineering of functional, perfusable 3D microvascular networks on a chip*. Lab on a Chip, 2013. **13**(8):p. 1489–1500.

[20] Moya, M. L., et al., *In vitro perfused human capillary networks*. Tissue Enineering Part C: Methods, 2013. **19**(9):p. 730–737.

[21] Jeon, J. S., et al., *Generation of 3D functional microvascular networks with human mesenchymal stem cells in microfluidic systems*. Integrative Biology, 2014. **6**(5):p. 555–563.

[22] Jeon, J. S., et al., *Human 3D vascularized organotypic microfluidic assays to study breast cancer cell extravasation*. Proceedings of the National Academy of Sciences, 2015. **112**(1):p. 214–219.

[23] Sobrino, A., et al., *3D microtumors in vitro supported by perfused vascular networks*. Scientific Reports, 2016. **6**.

[24] Hikimoto, D., et al., *High-Throughput Blood- and Lymph-Capillaries with Open-Ended Pores Which Allow the Transport of Drugs and Cells*. Advanced Healthcare Materials, 2016. **5**(15):p. 1969–1978.

[25] Sato, M., et al., *Microcirculation-on-a-chip: A microfluidic platform for assaying blood-and lymphatic-vessel permeability*. PLoS One, 2015. **10**(9):p. 1–18.

[26] Pisano, M., et al., *An in vitro model of the tumor–lymphatic*

microenvironment with simultaneous transendothelial and luminal flows reveals mechanisms of flow enhanced invasion. Integative Biology, 2015. **7**(5):p. 525–533.

[27] Xiong, Y., et al., *A robust in vitro model for trans-lymphatic endothelial migration*. Scientific Reports, 2017. **7**(1):p. 1633.

[28] Price, G. M., K. M. Chrobak, and J. Tien, *Effect of cyclic AMP on barrier function of human lymphatic microvascular tubes*. Microvascular Research, 2008. **76**(1):p. 46–51.

[29] Marino, D., et al., *Bioengineering Dermo-Epidermal Skin Grafts with Blood and Lymphatic Capillaries*. Science Translational Medicine, 2014. **6**(221):p. 221ra14-221ra14.

[30] Takeda, K., et al., *Adipose-derived stem cells promote proliferation, migration, and tube formation of lymphatic endothelial cells in vitro by secreting lymphangiogenic factors*. Annals of Plastic Surgery, 2015. **74**(6):p. 728–36.

[31] Strassburg, S., et al., *Adipose-Derived Stem Cells Support Lymphangiogenic Parameters In Vitro*. Journal of Cellular Biochemistry, 2016. **117**(11):p. 2620–2629.

[32] Gibot, L., et al., *Cell-based approach for 3D reconstruction of lymphatic capillaries in vitro reveals distinct functions of HGF and VEGF-C in lymphangiogenesis*. Biomaterials, 2016. **78**:p. 129–139.

[33] Knezevic, L., et al., *Engineering Blood and Lymphatic Microvascular Networks in Fibrin Matrices*. Frontiers in Bioengineering and Biotechnology, 2017. **5**.

[34] Kim, S., et al., *Three-dimensional biomimetic model to reconstitute sprouting lymphangiogenesis in vitro*. Biomaterials, 2016. **78**:p. 115–128.

[35] Chary, S. R., and R. K. Jain, *Direct measurement of interstitial convection and diffusion of albumin in normal and neoplastic tissues by fluorescence photobleaching*. Proceedings of the National Academy of Sciences, 1989. **86**(14):p. 5385–5389.

[36] Ng, C. P., B. Hinz, and M. A. Swartz, *Interstitial fluid flow induces myofibroblast differentiation and collagen alignment in vitro*. Journal of Cell Science, 2005. **118**(20):p. 4731–4739.

[37] Kelley, J., et al., *Cytokine signaling in lung: transforming growth factor-beta secretion by lung fibroblasts*. American Journal of Physiology-Lung Cellular and Molecular Physiology, 1991. **260**(2):p. L123–L128 .

[38] Wang, R., et al., *Hypertrophic scar tissues and fibroblasts produce more transforming growth factor□β1 mRNA and protein than normal skin and cells*. Wound Repair and Regeneration, 2000. 8(2):p. 128–137.

[39] Clavin, N. W., et al., *TGF-β 1 is a negative regulator of lymphatic regeneration during wound repair*. American Journal of Physiology-Heart and Circulatory Physiology, 2008. **295**(5):p. H2113–H2127,.

[40] Oka, M., et al., *Inhibition of endogenous TGF-β signaling enhances lymphangiogenesis*. Blood, 2008. **111**(9):p. 4571–4579.

초 록

림프계의 구성 요소인 림프관은 암세포와 면역세포의 주요 이동 통로로, 염증이나 전이와 같은 여러 질병들과 밀접하게 연결되어 있다. 하지만 지금까지 복잡한 체내 림프관 환경을 모사하는 적절한 체외 림프관 모델의 부재로 인하여 암의 전이 상황에서 림프관 기능의 기제를 밝히는데 어려움이 많았다. 따라서 이 연구에서는 미세 유세 소자를 이용해 관류가능한 관으로 이루어진 3차원 림프 전이 모델을 제시한다. 사람 유래의 림프내피세포와 섬유아세포, 그리고 림프 세포의 성장을 촉진시키는 여러 성장 인자들을 이용하면 미세 유체 소자 내에서 림프관이 만들어졌다. 또한 림프관 형성은 수압차에 의해 유도되는 적절한 속력의 유동에 의해 더욱 촉진되었다. 림프관은 림프내피세포와 섬유아세포가 각각 다른 채널에 패터닝될 때만 관류되었으며, 관류된 림프관은 기저막 구성 등 체내 림프관의 기본적인 특징들을 갖고 있음이 확인되었다. 림프관은 관류된 이후 성장 인자가 없는 배지에서도 5일 이상 기존의 상태를 유지했으며, 미세 유체 소자에 주입된 암세포는 관류된 림프관 내로 들어가 내벽에 안정적으로 달라붙었다. 이 연구는

미세 유체 소자를 이용해 간단하면서도 체내 림프관을 적절히 모사하는 3차원의 체외 림프관 모델을 제시하며, 제시된 모델은 암의 발전에서 림프관의 역할을 조사하고 림프관을 통한 암전이의 메커니즘을 알아내며 암 치료를 위한 약물 개발에 사용될 수 있을 것이다.

주요어: 림프관, 관류, 전이, 미세유체소자

학번: 2016-20656